European Journal of Pharmacology 790 (2016) 28–35

Contents lists available at ScienceDirect

European Journal of Pharmacology

journal homepage: www.elsevier.com/locate/ejphar

Technologies in kidney development or replacement

Upscaling of a living membrane for bioartificial kidney device

Natalia Vladimirovna Chevtchik [a], Michele Fedecostante [b], Jitske Jansen [b], Milos Mihajlovic [b], Martijn Wilmer [c], Marieke Rüth [d], Rosalinde Masereeuw [b], Dimitrios Stamatialis [a,*]

[a] Department of Biomaterials Science and Technology, MIRA Institute for Biomedical Technology and Technical Medicine, University of Twente, Enschede, The Netherlands
[b] Department of Pharmaceutical Sciences, UIPS Institute for Pharmaceutical Sciences, Utrecht University, Utrecht, The Netherlands
[c] Department of Pharmacology and Toxicology, Radboud Institute for Molecular Life Sciences, Radboudumc, Nijmegen, The Netherlands
[d] eXcorLab GmbH, Industrie Center Obernburg, Obernburg, Germany

ARTICLE INFO

Article history:
Received 31 March 2016
Received in revised form
24 June 2016
Accepted 6 July 2016
Available online 6 July 2016

Keywords:
Bioartificial kidney device
Living membrane
Functionalized hollow fiber membranes
Conditionally immortalized human renal proximal tubule epithelial cells
Monolayer of functional cells

ABSTRACT

The limited removal of metabolic waste products in dialyzed kidney patients leads to high morbidity and mortality. One powerful solution for a more complete removal of those metabolites might be offered by a bioartificial kidney device (BAK), which contains a hybrid "living membrane" with functional proximal tubule epithelial cells (PTEC). These cells are supported by an artificial functionalized hollow fiber membrane (HFM) and are able to actively remove the waste products. In our earlier studies, conditionally immortalized human PTEC (ciPTEC) showed to express functional organic cationic transporter 2 (OCT2) when seeded on small size flat or hollow fiber polyethersulfone (PES) membranes. Here, an upscaled "living membrane" is presented. We developed and assessed the functionality of modules containing three commercially available MicroPES HFM supporting ciPTEC. The HFM were optimally coated with L-Dopa and collagen IV to support a uniform and tight monolayer formation of matured ciPTEC under static culturing conditions. Both abundant expression of zonula occludens-1 (ZO-1) protein and limited diffusion of FITC-inulin confirm a clear barrier function of the monolayer. Furthermore, the uptake of 4-(4-(dimethylamino)styryl)-N-methylpyridinium iodide (ASP^+), a fluorescent OCT2 substrate, was studied in absence and presence of known OCT inhibitors, such as cimetidine and a cationic uremic solutes mixture. The ASP^+ uptake by the living upscaled membrane was decreased by 60% in the presence of either inhibitor, proving the active function of OCT2. In conclusion, this study presents a successful upscaling of a living membrane with active organic cation transport as a support for BAK device.

1. Introduction

Within the growing worldwide population of kidney patients undergoing dialysis treatment, mortality (15–20% per year) and morbidity remain high (Vanholder et al., 2003a). One of the reasons could be the limited removal of protein-bound retention solutes (Krieter et al., 2009; Meyer et al., 2005). Their accumulation is strongly associated with the fatal outcome in the patients (Vanholder et al., 2014). In the functional kidney, proximal tubule epithelial cells (PTEC), equipped with a broad range of transporters, mediate the excretion of those solutes. One of the PTEC transporters involved in the excretion of cationic uremic metabolites and drugs is the basolateral organic cation transporter – 2 (OCT2; *SLC22A2*) (Schophuizen et al., 2013).

The development of a PTEC-based bioartificial kidney (BAK) device could improve existing dialysis therapies for the removal of protein-bound uremic retention solutes (Jansen et al., 2014a; Vanholder et al., 2003a). A key requirement for a BAK is the formation of a "living membrane" consisting of a tight monolayer of renal cells with preserved functional organic ion transporters, grown on an artificial porous hollow fiber membrane (HFM). One side of these HFM need to be highly haemocompatible since it would be in contact with blood, whereas the other side should be bioactive to support the formation of a cell monolayer.

Several groups have presented their achievements in upscaled

Abbreviations: ASP^+, 4-(4-(dimethylamino)styryl)-N-methylpyridinium iodide; BAK, bioartificial kidney device; BSA, bovine serum albumin; ciPTEC, conditionally immortalized human proximal tubule epithelial cells; CWF, clean water flux; ECM, extracellular matrix; HBSS, Hank's balanced salt solution; HFM, hollow fiber membrane; IgG, immunoglobulin G; Inulin-FITC, fluorescein isothiocyanate (FITC)-labelled-inulin; KHH, Krebs-Henseleit buffer supplemented with HEPES (10 mM); L-Dopa, 3,4-dihydroxy-L-phenylalanine; PES, polyethersulfone; PTEC, proximal tubule epithelial cell; SEM, scanning electron microscopy; SC, sieving coefficient; UT mix, uremic toxin mix; ZO-1, zonula occludens-1

* Corresponding author.
E-mail address: d.stamatialis@utwente.nl (D. Stamatialis).

http://dx.doi.org/10.1016/j.ejphar.2016.07.009
0014-2999/

BAK systems in recent years (Humes et al., 2014; Saito et al., 2011; Tasnim et al., 2010). In terms of materials for the HFM, Polyethersulfone (PES), polysulfone (PSF), polyacrylonitrile (PAN) and cellulose acetate membranes have mostly been evaluated (Ni et al., 2011). Those materials were chosen for their good haemocompatibility properties and limited fouling, and therefore had to be functionalized by various extracellular matrix (ECM) components, such as laminin, polylysine, pronectin, gelatin, or collagen IV (Ni et al., 2011; Schophuizen et al., 2015; Zhang et al., 2009). As for the renal cell lines, the ones originating from humans are preferred to those from other species (Shitara et al., 2006; Tahara et al., 2005). Several groups showed the presence of various markers, indicating that the cells preserved their phenotype (Oo et al., 2011) without characterizing their function (Humes et al., 2004; Oo et al., 2011, 2013; Sanechika et al., 2011; Zhang et al., 2009). Moreover, the most important drawbacks of primary cells are limited availability, low proliferative capacity and donor-to-donor variation.

To overcome these drawbacks, the recently developed and well-characterized conditionally immortalized human PTEC line (ciPTEC) is a suitable candidate to develop an efficient BAK system (Jansen et al., 2014b; Wilmer et al., 2010). The ciPTEC were transduced with human telomerase (hTERT) that limits replicative senescence by telomere length maintenance. In addition, their proliferation is controlled by the temperature sensitive vector SV40tsA58, allowing proliferation at 33 °C and differentiation in mature PTEC at 37 °C. Two of our recent studies proved the concept of using the PTECs for BAK application. In fact, when the cells were cultured on bioactive Polyethersulfone (PES)-based flat sheet membranes (Schophuizen et al., 2015) or small size hollow fibers (Jansen et al., 2015), they presented functional OCT2.

In this work, we investigated the upscaling of this concept and developed modules containing three "living membranes". The transport properties of the polymeric membrane and the quality and function of the grown ciPTEC monolayer were systematically investigated, including the expression of zonula occludens-1 (ZO-1) protein and the diffusion of fluorescein isothiocyanate (FITC)-labelled-inulin (inulin-FITC). Moreover, we also studied the uptake of a specific fluorescent OCT substrate in the presence or absence of the OCT inhibitors (Schophuizen et al., 2013).

2. Materials and methods

2.1. Chemicals

All chemicals were purchased from Sigma-Aldrich (Zwijndrecht, The Netherlands) unless stated otherwise. MicroPES TF10 hollow fiber capillary membranes (HFM) (wall thickness 100 μm, inner diameter 300 μm, max pore size 0.5 μm) were purchased from 3M – Membrana GmbH (Wuppertal, Germany). CiPTEC were cultured as described previously (Wilmer et al., 2010).

2.2. Module preparation

MicroPES HFM were mounted into mini modules composed of Kartell PP T-shaped connectors (Fisher Scientific, Landsmeer, the Netherlands) and PE rigid semi-transparent tubing diameter 6–8 mm (VWR International B.V, Amsterdam, the Netherlands), see Fig. 1. The modules were potted with polyurethane bi-component resin (Intercol B. V, Ede, the Netherlands), allowed to dry for at least 24 h, and cut open. To ensure further ease of use of the modules, we added Luer Lock fittings and caps (Cole Palmer, Metrohm Applikon BV, Schiedam, the Netherland) to the inlets and outlets, and connected them together using silicon tubing (VWR International B. V, Amsterdam, the Netherlands). Three fibers were

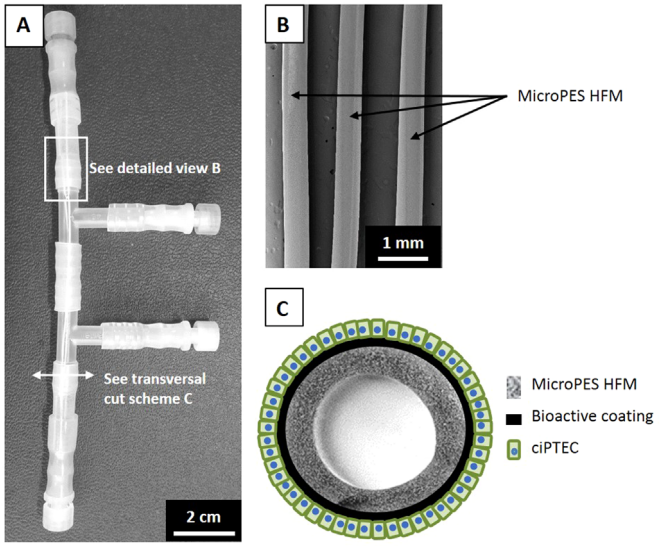

Fig. 1. *Upscaled "living membrane".* (A) Picture of one module used for upscaled "living membrane" model. Three MicroPES hollow fiber membranes (HFM) within a housing composed of PE, PP and silicone parts, Luer Lock fittings and caps. (B) SEM image of three MicroPES HFM. (C) Scheme of a transversal cut of one "living membrane". Not at proportional scale.

mounted in every module, with an effective length of 8.5 ± 0.5 cm and a surface of 4.01 ± 0.25 cm^{-2} available for cell seeding. After cell seeding, extra luminary inlets were supplemented with gas exchange Sartorius Minisart sterile filters (Fisher Scientific, Landsmeer, the Netherlands).

2.3. Membrane sterilization and coating

The bioactive coating was performed on the extraluminal side of the HFM, with slight modifications to the previously established methods (Jansen et al., 2015; Ni et al., 2011). The modules were sterilized using 70% (v/v) EtOH incubation for one h, washed and incubated using sterile 10 mM Tris buffer (pH 8.5) for 1 h. The primary coating component L-Dopa (L-3,4-dihydroxyphenylalanine, 2 mg ml^{-1}) was dissolved in Tris buffer at 37 °C for 45 min. The L-Dopa solution was sterile filtered and injected in the extraluminal space of the module, completely filling it. The primary coating was performed at 37 °C, on a shaking device, for 20 h. Afterwards, the L-Dopa solution was removed; the modules were washed with Hank's balanced salt solution (HBSS) (Fisher Scientific, Landsmeer, the Netherlands) buffer and filled with the second coating component – human collagen IV (25 μg ml^{-1} in HBSS). The coating with collagen IV was performed at 37 °C, on a shaking device, for 2 h. Finally, the collagen IV solution was removed and the modules were washed with HBSS.

2.4. Membrane characterization

The membrane topography of both uncoated and coated HFM was visualized using scanning electron microscopy (SEM), as described previously (Jansen et al., 2015; Schophuizen et al., 2015). We used an OSMO Inspector automated setup (Convergence B. V, Enschede, The Netherlands) to quantify the transport of pure water (Merck Millipore, Billerica, MA) and PBS solutions with 1 mg/ml bovine serum albumin (BSA) and 0.02 mg/ml immunoglobulin G (IgG) solutions through the uncoated and coated cell-free HFMs. The flux through the membranes (J, in l m^{-2} h^{-1}) was plotted as a function of the Transmembrane Pressure (ΔP, in bar). The permeance (L, in l m^{-2} h^{-1} bar^{-1}) was calculated from the slope of this curve. Every pressure step was maintained for

30 min. The sieving coefficients (SC) for BSA and IgG were determined by dividing the concentration of these proteins in the permeate by their concentration in the feed protein solution. BSA and IgG concentrations were measured by spectrophotometric analysis (Agilent Technologies, Cary 300 UV–vis system) using quartz cuvettes at 280 nm.

2.5. Cell culture

The ciPTEC cell line (Wilmer et al., 2010) was cultured at a 33 °C proliferating temperature in a ciPTEC complete medium prepared as follows: phenol red free Dulbecco's modified Eagle medium DMEM-HAM's F12 (Lonza; Basel, Switzerland) was supplemented with 10% v/v foetal calf serum (FCS; Greiner Bio-One; Alphen a/d Rijn, The Netherlands), insulin, transferrin, selenium (ITS; I=5 μg/ml; T=5 μg/ml; S=5 ng/ml), 36 ng/ml hydrocortisone, 10 ng/ml epidermal growth factor and 40 pg/ml tri-iodothyronine. Antibiotics were added to the medium only in the proliferating culture. During maturation at 37 °C, the culture media were antibiotic free. CiPTEC were cultured up to a maximum of 40 passages, during which the proximal tubular characteristics remain unaltered (Wilmer et al., 2010).

2.6. HFM modules handling

Prior to cell seeding, modules were incubated for 1 h in ciPTEC complete medium. Proliferating 90% confluent ciPTEC were detached using Accutase (StemPro® Accutase®, Life Technologies Europe BV, Bleiswijk, the Netherlands), centrifuged and suspended at 2.5 million cells/ml density in the ciPTEC complete medium. The modules' extraluminal space was completely filled with the cell suspension. To promote initial cell attachment, the modules were placed at 33 °C, 5% CO_2 for 8 h, with a rotation of 90° every 2 h. Afterwards, modules were washed with the ciPTEC complete medium, provided with gas exchange filters and cellular proliferation was allowed for additional 64 h. Finally, the temperature was changed to 37 °C for 7 days to promote the formation of a differentiated monolayer. During the whole culture period, ciPTEC were supplemented with fresh culture media every day.

2.7. Immunochemistry

The expression of OCT2, zonula occludens-1 (ZO-1) in ciPTEC monolayers on hollow fibers were investigated using the immunocytochemistry methodology as previously described (Jansen et al., 2014b) and examined under the Nikon confocal A1/ super resolution N-STORM microscope (Nikon Instruments Europe B.V, Amsterdam, The Netherlands). Images were captured using the NIS-elements analysis software, version 4.40.000.

2.8. Transepithelial barrier function

Paracellular permeability was quantified in the living membranes following the previously described method (Jansen et al., 2015). Shortly: after washing the modules with Krebs-Henseleit buffer supplemented with HEPES (10 mM; KHH buffer), inulin-FITC (0.1 mg ml^{-1} in KHH buffer) was perfused at 18 ml h^{-1} at 37 °C for 15 min. The fluorescence of the samples and of a standard range of concentrations was measured using a Tecan infinite M200PRO plate reader (Tecan Austria GmbH) at an excitation wavelength of 485 nm and an emission wavelength of 535 nm. Coated and uncoated HFM without cells were used as negative controls. The flux of inulin-FITC (J) was calculated in pM min^{-1} cm^{-2}, using an average molar mass of 4500 mg/mM for inulin-FITC.

2.9. Functional organic cation transport

The activity of OCT2 was evaluated by perfusing the modules with the fluorescent substrate 4-(4-(dimethylamino)styryl)-N-methylpyridinium iodide (ASP^+, 10 μM) in KHH buffer, at 18 ml h^{-1} at 37 °C for 30 min. The assay was performed in the presence or absence of a cationic uremic toxin mix (UT mix; 10 times the uremic plasma concentrations reported in the literature (Schophuizen et al., 2013)) or cimetidine (100 μM). After perfusion, the modules were washed with KHH buffer and fixed for 30 min in a fixing solution (4% Sucrose, 2% Paraformaldehyde in HBSS).

The modules were carefully cut open and the extracted fibers were mounted on microscopy slides using Dako fluorescent mounting media (Dako Netherlands B.V, Heverlee, Belgium). Slides were directly analysed at a constant laser intensity using the Nikon confocal A1/ super resolution N-STORM microscope. Images were captured using the NIS-elements analysis software (version 4.40.000) and quantification of the data was performed using ImageJ software (ImageJ 1.40 g, NIH, USA). The average pixel intensities of four cells in the focal plan were extracted for the various conditions.

2.10. Data analysis

Every experiment was performed at least in duplicate. The number of samples (n) measured is indicated and presented in each figure legend. The results are presented as mean ± standard deviation. Statistical analysis was performed in the SPSS software (IBPM SPSS Statistics version 23.0) using a one-way analysis of variance (ANOVA) or Student's *t*-test, where appropriate. A P-value of < 0.05 was considered significantly different.

3. Results

3.1. Membrane characterization

The surface of MicroPES HFM was functionalized via a double coating to allow the formation of a tight homogeneous cell monolayer. This coating was successfully used on a flat PES membrane (Schophuizen et al., 2015) and then on a single small (1–2 cm long) HFM (Jansen et al., 2015). Here, we performed the coating on the upscaled system of three HFM with a total surface area of 4 ± 0.25 cm^2. Some previous studies (Kandasamy et al., 2014) and preliminary experiments with shorter coating time (data not shown) suggested that a prolonged coating of membranes is necessary to generate a reliable and reproducible cell monolayer. Therefore, the previously optimized L-Dopa coating time was extended until 20 h instead of 5 h (on small HFM) (Jansen et al., 2015) or a few min (on flat membranes) (Schophuizen et al., 2015). The collagen IV coating time was also extended to 2 h instead of 1 h as was done previously (Jansen et al., 2015).

Fig. 2 compares the SEM images of the surface and cross-sections of uncoated and coated HFM in the absence of cells. Although we applied a longer coating time for L-Dopa, the pores remain open. The slight colour difference between uncoated and coated HFM is due to the charge of the sample during SEM analysis and does not reflect the coating state.

The effect of the coating on the membrane transport properties was measured by clean water and proteins transport experiments. Fig. 3A shows the clean water flux (CWF) through the uncoated or coated HFM at different pressures and Fig. 3B shows the SC of BSA and IgG at the same pressure range. The clean water permeance of the coated membranes ($(10.6 \pm 1.7) \cdot 10^3$ l m^{-1} h^{-1} bar^{-1}) is lower ($P < 0.001$) than the permeance of the uncoated membranes, ($(18.2 \pm 1.9) \cdot 10^3$ l m^{-1} h^{-1} bar^{-1}) but is still very high.

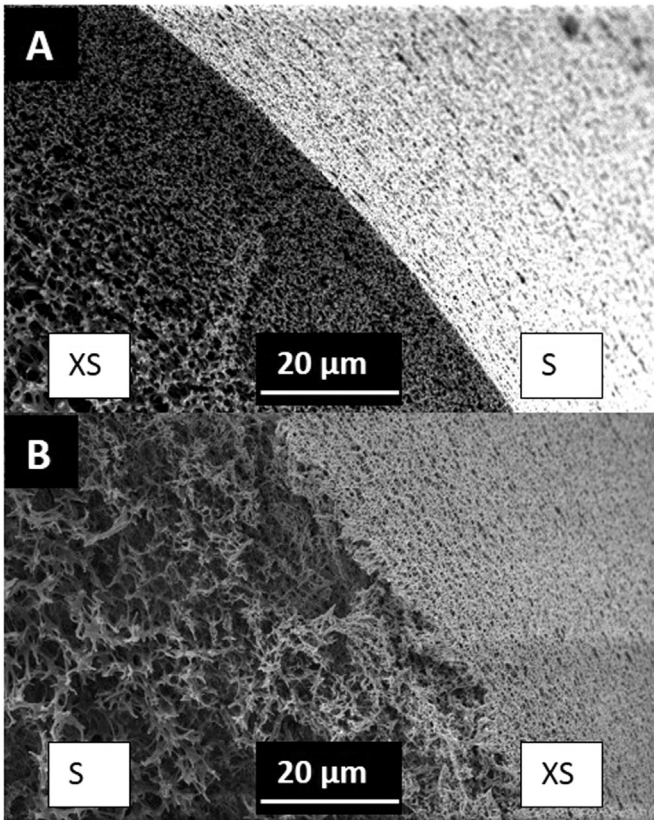

Fig. 2. *SEM images of MicroPES HFM.* (A) uncoated and (B) with L-Dopa and collagen IV double coating.

These results are consistent with the SEM observation that the pores of the coated membranes are open (Fig. 1B). Besides, BSA with a molecular weight ~66 kDa still passes freely through the coated membrane, as demonstrated by the SC (0.99 ± 0.00 versus 0.98 ± 0.01), Fig. 3B. The passage of a larger protein molecule, IgG (molecular weight ~166 kDa), is partially affected (SC 0.79 ± 0.04 versus 0.97 ± 0.02 for the uncoated HFM, $P < 0.001$). These results indicate a slight decrease in the pore size caused by the prolonged coating.

3.2. Cell monolayer integrity

Fig. 4 shows representative images of ciPTEC cultured on MicroPES HFM. Only a few cells can be found on the uncoated HFM (Fig. 4A). The L-Dopa (5 h) and collagen IV (1 h) double coating strongly improves cellular adhesion of the ciPTEC (Fig. 4B), but does not lead to the formation of a complete cell monolayer. The prolonged L-Dopa (20 h) and collagen IV (2 h) coating allows the formation of a uniform ciPTEC monolayer (Fig. 4C and D). In this condition, the abundant expression of the Zonula Occludens 1 (ZO-1) protein along the cell boundaries confirms the presence of tight junctions between the cells. In addition to a polarized epithelial barrier, the tight junction proteins contribute to fluid and ion homeostasis mediated by paracellular transport (Kirk et al., 2010). This tight cell monolayer is present on the whole length of the HFM within a module and is achieved for all three HFM (data not shown).

Fig. 4E shows the paracellular leakage of inulin-FITC as mean ± standard deviation of three experiments performed at least in triplicate. Since no active transcellular transport has been reported for inulin-FITC, its paracellular leakage was used an indicator of passive diffusion and thus monolayer tightness (Schophuizen et al., 2015). When compared to the uncoated or coated HFM without cells, the coated HFM with renal cell monolayer presents a low inulin-FITC leakage (778 ± 56 pM min^{-1} cm^{-2} and 812 ± 2 pM min^{-1} cm^{-2} vs 301 ± 103 pM min^{-1} cm^{-2}, respectively ($P < 0.001$ using an unpaired *t*-test)). Consistent with the previous microscopy data, the paracellular low inulin-FITC leakage confirms formation of a tight ciPTEC monolayer.

3.3. Cell function – ASP^+ uptake

To further examine the functionality of the matured ciPTEC monolayers grown on functionalized HFM modules, we assessed the activity of OCT2, which is expressed along the basolateral membrane of PTEC. This transporter is responsible for the uptake of cationic uremic metabolites (Schophuizen et al., 2013) and may be crucial for their renal elimination. Here, we perfused the HFM modules intraluminally with ASP^+, an OCT2 fluorescent substrate, in the absence or presence of competitive inhibitors of OCT2 mediated uptake: either uremic cationic toxin mix or cimetidine (Schophuizen et al., 2013). Fig. 5A shows representative confocal images of the three conditions. The uptake of the ASP^+ alone gives

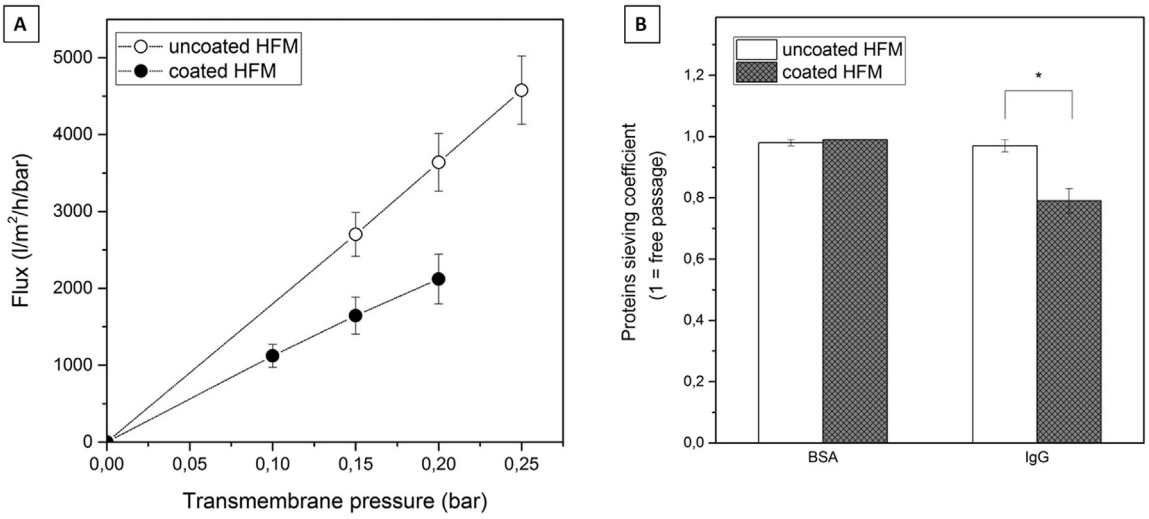

Fig. 3. *HFM transport properties.* (A) Clean water fluxes (CWF) and (B) sieving coefficients of bovine serum albumin (BSA) and immunoglobulinG (IgG) for uncoated and coated HFM. (A) The slope of the CWF as a function of the pressure gives the membrane permeance. Data are shown as mean ± standard deviation of three samples per case. * $P < 0.001$ using an unpaired *t*-test.

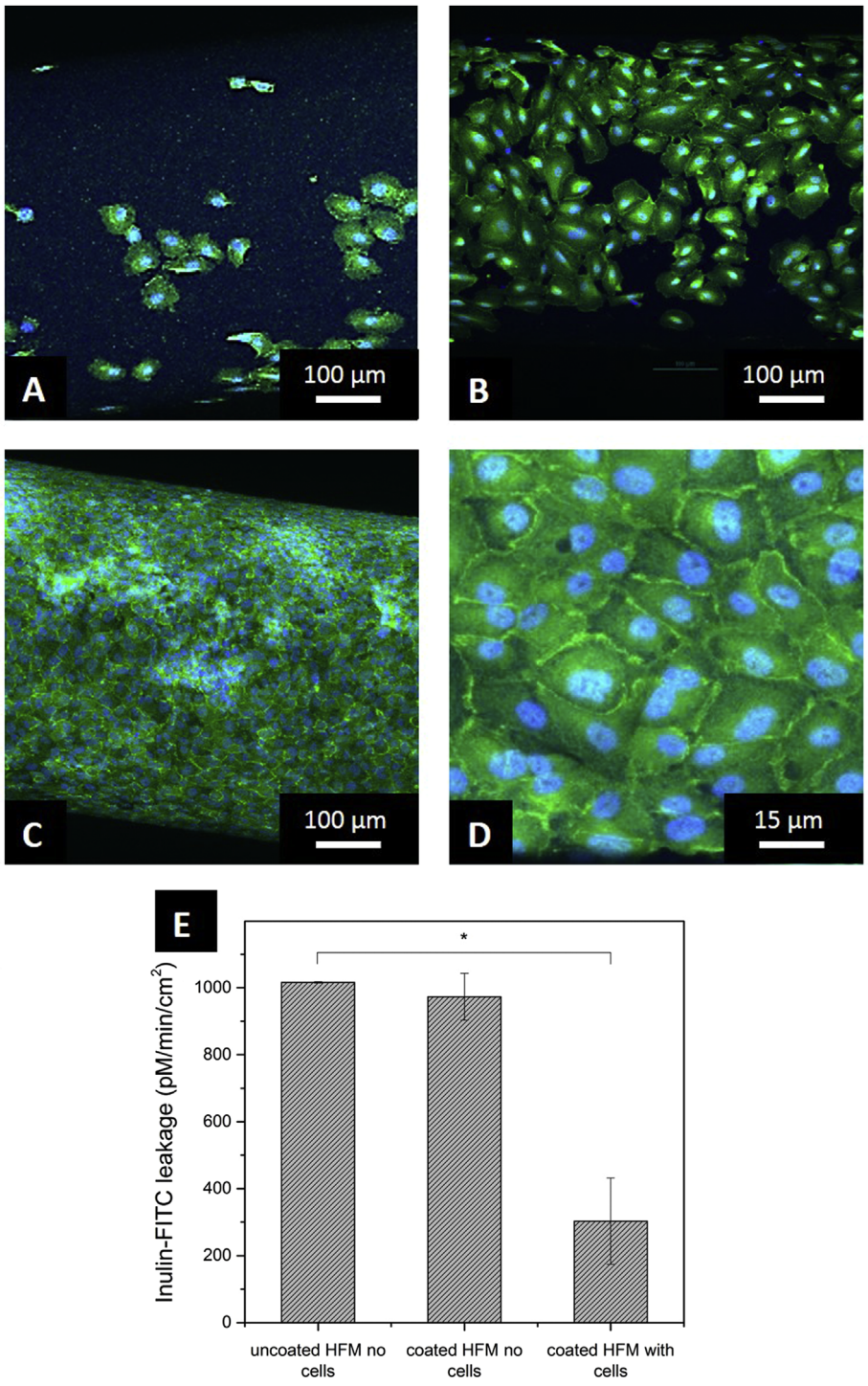

Fig. 4. *Monolayer quality of ciPTEC cultured on HFM.* (A, B, C, D) Representative confocal microscopy images of ciPTEC cultured on HFM with in blue the DAPI staining of nuclei and in green the immunostaining for ZO-1 (A, B, C, D). (E) Inulin-FITC paracellular leakage. A – Uncoated HFM. B – HFM with short coating time. C and D – HFM with optimal coating time. Data are presented as the mean ± standard deviation of at least 4 samples. *$P < 0.001$ using an unpaired *t*-test. (For interpretation of the references to color in this figure legend, the reader is referred to the web version of this article).

a strong fluorescent signal, which is significantly reduced in presence of either uremic toxin mix or cimetidine (Fig. 5B). The intensity of the fluorescent signal in presence of inhibitor is normalized to the signal of the uptake of the ASP^+ alone, after 30 min of perfusion. The ASP^+ uptake is inhibited by ~60% by both uremic cationic toxin mix and cimetidine (39% and 36% of the original intensity, respectively), confirming a functional monolayer is created on double-coated HFM in the modules.

4. Discussion

In this study, we developed upscaled modules of "living membranes" for BAK with a functional ciPTEC monolayer grown on coated MicroPES HFM. The double coating of L-Dopa and collagen IV was thin and preserved the membrane transport properties. The cells formed homogeneous monolayers with well-expressed ZO-1 protein and low paracellular leakage. As proof of concept, the

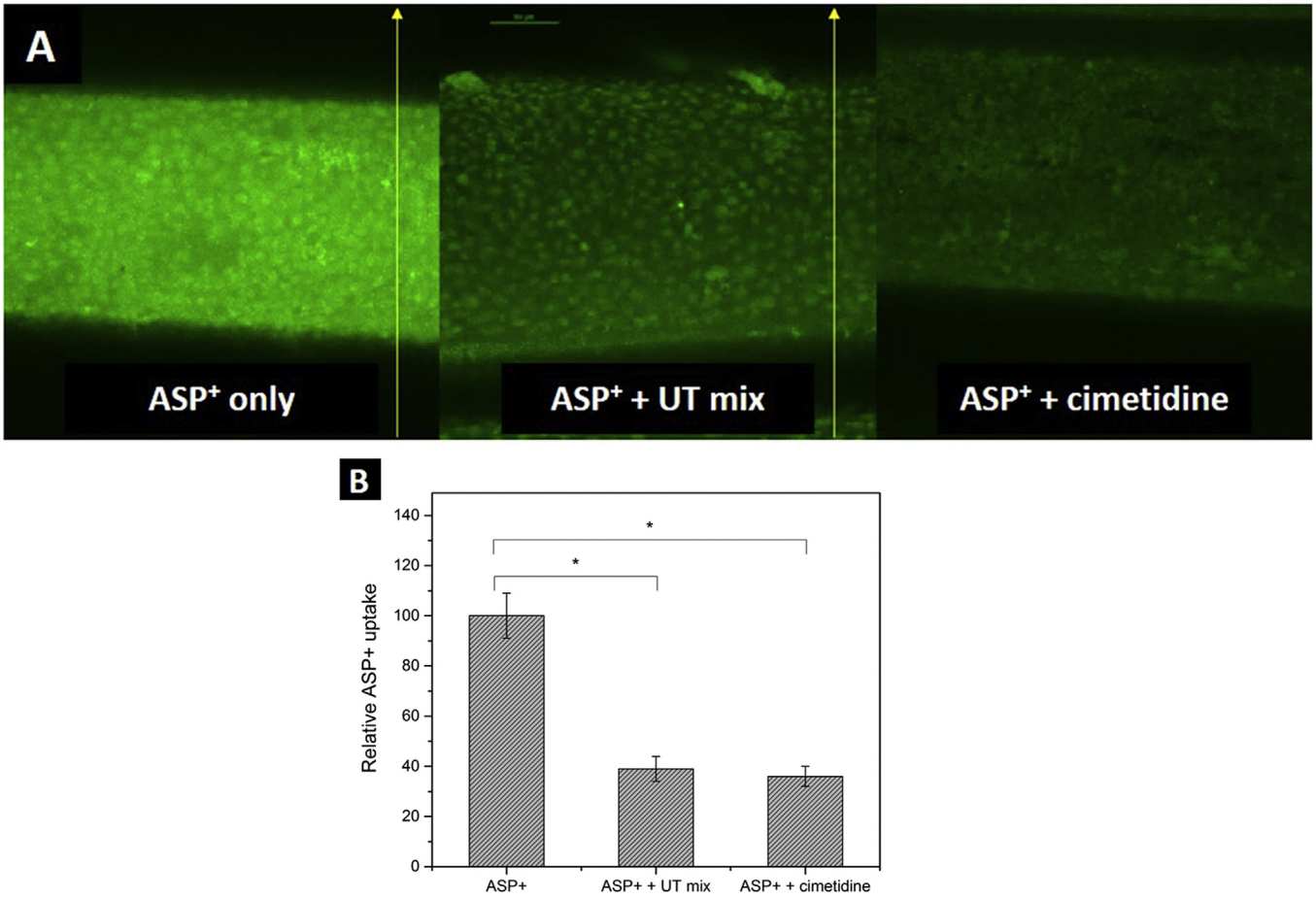

Fig. 5. *Functional organic cation transporter-2 transport.* (A) Representative confocal microscopy images and (B) quantification of ASP^+ uptake (10 μM) in the absence or presence of specific inhibitors (cationic uremic toxin mix (UT mix), cimetidine (cim, 100 μM)) in matured ciPTEC cultured on upscaled HFM. The perfusion lasted for 30 min. Data are normalized against ASP^+ uptake in the absence of inhibitors and presented as mean ± standard deviation of four measurements of the intensity of four cells in the projection plan, from two HFM containing modules. *$P < 0.001$ using ANOVA.

obtained ciPTEC monolayers demonstrated active uptake a specific OCT substrate, demonstrative of the successful upscaling of a "living membrane" suitable for a BAK device.

The MicroPES membrane is designed for plasma fractionation and, therefore, has antifouling properties. Hence, it does not promote cell adhesion and requires a functionalization on the extraluminal side. The first coating component – L-Dopa – is enriched in mussel-like adhesive proteins and can adhere to a wide range of surfaces (Lee et al., 2007). The second coating component – collagen IV – is an essential positively charged component of the extracellular matrix of renal tubular epithelial cells and has previously been successfully used, in combination with the negatively charged L-Dopa, to establish a PTEC monolayer both for primary cells (Oo et al., 2011) and ciPTEC (Schophuizen et al., 2015). To support the growth of ciPTEC on the outer surface of the HFM (4 cm^2), this double coating, initially applied for a few min for PES flat membranes (Schophuizen et al., 2015), has been later applied for several h (5 h L-Dopa +1 h collagen IV) for single fiber HFM (0.13 cm^2) (Jansen et al., 2015). However, when such coatings were applied in our module system, no reproducible monolayer could be obtained (Fig. 4B). We had to prolong the L-Dopa coating to 20 h, and therefore came closer to the coating conditions previously applied for primary renal cells (Oo et al., 2011). As to the collagen IV, the coating was also extended to obtain the desired deposition pattern to promote the initial cell adhesion. Moreover, a low speed dynamic regime during the L-Dopa coating (shaking or low flow) was applied to ensure a good homogeneity of the coating on the whole membrane length and within all the HFM of the same module.

The double coating seems to decrease the membrane pore size as shown by the clean water flux and the sieving of BSA and IgG experiments. However, the transport though the membrane is still high, allowing transport of nutrients and toxins. Compared to the previous study with the small HFM (Jansen et al., 2015), both clean water permeance and IgG sieving coefficients are decreased ($(10.6 \pm 1.7) \cdot 10^3$ l m^{-1} h^{-1} bar^{-1} versus $(16.4 \pm 0.7) \cdot 10^3$ l m^{-1} h^{-1} bar^{-1} and 0.79 ± 0.04 versus 0.90 ± 0.01 respectively). The fact that both BSA and IgG can pass through the HFM and reach the ciPTEC monolayer should not be detrimental for a BAK application, since the ciPTEC tight monolayer is intended to form the functional barrier against the loss of essential proteins by the patient. Besides, the transport of albumin through the membrane towards the ciPTEC monolayer may be advantageous for the elimination protein bound compounds (Vanholder et al., 2003a), since those need to be in close proximity to the cell transporters.

The ciPTEC monolayer was characterized after 7 days of maturation at 37 °C in the upscaled modules. The confocal microscopy shows regular nuclei, homogeneous cell shapes and abundant expression of the tight junction protein ZO-1. This underlines the epithelial character of the ciPTEC monolayer, which is confirmed further by low inulin-FITC diffusion. When compared to the results obtained for the single HFM (Jansen et al., 2015), the inulin transport through the HFM both with and without cells is similar (without cells: 973 ± 70 pM min^{-1} cm^{-2} now compared to 1200 ± 193 pM min^{-1} cm^{-2} previously; with cells: 303 ± 129 pM min^{-1} cm^{-2} now compared to 373 ± 42 pM min^{-1} cm^{-2} previously). A similar range of

inulin-FITC permeability was found earlier in vitro, too (Ferrell et al., 2010). Apparently, the longer coating time in this study (versus the small scale HFM) does not affect the inulin diffusion (973 ± 70 pM min^{-1} cm^{-2} for the coated HFM versus 1016 ± 2 pM min^{-1} cm^{-2} for the uncoated HFM). This result was to be expected since the inulin-FITC is much smaller than BSA (inulin has a molecular weight of ~4.5 kDa and BSA has one of ~66 kDa), which passes freely through the membrane. Finally, the high standard deviation (303 ± 129 pM min^{-1} cm^{-2} Fig. 4) obtained for the HFM with cell monolayer may suggest some local irregularities in the epithelial barrier due to the more complex handling and characterizing procedures. In other studies, intraluminal seeding of the PTEC was preferred (Humes et al., 2002; Saito et al., 2012; Tasnim et al., 2010) and required an inverted design of the HFM, with a selective layer on the extraluminal wall to avoid pore clogging (Oo et al., 2011). Though the extraluminal cell seeding has been reported less frequently (Oo et al., 2013), it allows the use of commercial HFM designed for plasma fractionation, having the selective layer on the intraluminal wall. This, together with the compatibility with our imaging techniques, justifies the configuration used here.

Finally, our upscaled system can preserve the functionality of the OCT-2 of the ciPTEC monolayer, which is crucial to ensure the clearance of cationic uremic solutes (Vanholder et al., 2003b; Zolk et al., 2009) in a BAK application. We analysed the uptake of the specific fluorescent substrate ASP^+ and its inhibition in the presence of a polyamine and guanidino cationic uremic toxin mixture (Schophuizen et al., 2013), as well as in the presence of cimetidine (Fujita et al., 2006; Kido et al., 2011; Urakami, 2002). The intensity of the intracellular fluorescence signal corresponding to the ASP^+ uptake alone is very strong (Fig. 5A). This intensity decreases dramatically in presence of either inhibitor. The inhibitory effect of the uremic toxin mixture observed here, is slightly stronger than that for a small fiber (Jansen et al., 2015), probably due to either the prolonged uptake time (30 min instead of 13 min), or the system upscaling (4.01 cm^2 against 0.13 cm^2 previously). Indeed, in the upscaled system, 4.01 cm^2 of cells received daily 2.5 ml of medium. The small HFM were cultured in 6 well plates, and thus 0.13 cm^2 of cells were receiving 2.5 ml of medium every 2 or 3 days. In order to compare more accurately both systems, complete analysis should be performed at several time points.

5. Conclusion and outlook

This work presents the upscaling of a "Living Membrane" comprising of functionalized MicroPES HFM supporting ciPTEC. This Living Membrane, developed under static culturing conditions, exhibits a uniform, reproducible and tight ciPTECs monolayer. Our work shows that PTEC cultured in this upscaled system feature active organic cationic transport, crucial for the removal of uremic cationic metabolites.

The next step towards a functional BAK device is to culture the cells while exposing them to a unidirectional flow with relative shear stress to mimic the natural kidney proximal tubule physiology. There is evidence (Weinbaum et al., 2010) the ciPTEC brush-border barrier height and therefore surface available for uremic metabolites uptake increases significantly when culturing cells under shaking conditions in a 2D environment. This result, supported by similar evidence for other cell lines (Jang et al., 2013; Kim et al., 1998; Li and Cui, 2014; Sánchez-Romero et al., 2016), suggests better toxin removal under dynamic conditions. Finally, a ciPTEC-based BAK device should also ensure a sufficient toxin clearance for a prolonged session. Here, the upscaled "living membrane" has been tested for 30 min. Therefore future work should evaluate longer clearance periods.

Acknowledgements

This work was funded by the EU Marie Curie ITN Project BIOART (grant no. 316690 and EU-FP7-PEOPLE-ITN-2012). Dimitrios Stmatialis would like to gratefully thank the EUTox Working Group, of the European society of European Society for artificial organs for its financial contribution. Natalia V. Chevtchik would like to gratefully thank the BioNanoLab of the University of Twente, the Netherlands for its financial contribution. The authors would like to gratefully thank Felix Broens and Convergence Industry B.V. for the technical assistance in the program development for membrane properties characterisation.

References

Ferrell, N., Desai, R.R., Fleischman, A.J., Roy, S., Humes, H.D., Fissell, W.H., 2010. A microfluidic bioreactor with integrated transepithelial electrical resistance (TEER) measurement electrodes for evaluation of renal epithelial cells. Biotechnol. Bioeng. 107, 707–716.

Fujita, T., Urban, T.J., Leabman, M.K., Fujita, K., Giacomini, K.M., 2006. Transport of drugs in the kidney by the human organic cation transporter, OCT2 and its genetic variants. J. Pharm. Sci. 95, 25–36.

Humes, H.D., Buffington, D., Westover, A.J., Roy, S., Fissell, W.H., 2014. The bioartificial kidney: current status and future promise. Pediatr. Nephrol. 29, 343–351.

Humes, H.D., Fissell, W.H., Weitzel, W.F., Buffington, D.A., Westover, A.J., MacKay, S. M., Gutierrez, J.M., 2002. Metabolic replacement of kidney function in uremic animals with a bioartificial kidney containing human cells. Am. J. Kidney Dis. 39, 1078–1087.

Humes, H.D., Weitzel, W.F., Bartlett, R.H., Swaniker, F.C., Paganini, E.P., Luderer, J.R., Sobota, J., 2004. Initial clinical results of the bioartificial kidney containing human cells in ICU patients with acute renal failure. Kidney Int. 66, 1578–1588.

Jang, K.J., Mehr, A.P., Hamilton, G.A., McPartlin, L.A., Chung, S., Suh, K.Y., Ingber, D.E., 2013. Human kidney proximal tubule-on-a-chip for drug transport and nephrotoxicity assessment. Integr. Biol.: Quant. Biosci. Nano Macro 5, 1119–1129.

Jansen, J., Fedecostante, M., Wilmer, M.J., van den Heuvel, L.P., Hoenderop, J.G., Masereeuw, R., 2014a. Biotechnological challenges of bioartificial kidney engineering. Biotechnol. Adv. 32, 1317–1327.

Jansen, J., Schophuizen, C.M., Wilmer, M.J., Lahham, S.H., Mutsaers, H.A., Wetzels, J. F., Bank, R.A., van den Heuvel, L.P., Hoenderop, J.G., Masereeuw, R., 2014b. A morphological and functional comparison of proximal tubule cell lines established from human urine and kidney tissue. Exp. Cell Res. 323, 87–99.

Jansen, J., De Napoli, I.E., Fedecostante, M., Schophuizen, C.M., Chevtchik, N.V., Wilmer, M.J., van Asbeck, A.H., Croes, H.J., Pertijs, J.C., Wetzels, J.F., Hilbrands, L. B., van den Heuvel, L.P., Hoenderop, J.G., Stamatialis, D., Masereeuw, R., 2015. Human proximal tubule epithelial cells cultured on hollow fibers: living membranes that actively transport organic cations. Sci. Rep. 15, 16702. http://dx.doi.org/10.1038/srep16702, 2015.

Kandasamy, K., Narayanan, K., Ni, M., Du, C., Wan, A.C., Zink, D., 2014. Polysulfone membranes coated with polymerized 3,4-dihydroxy-L-phenylalanine are a versatile and cost-effective synthetic substrate for defined long-term cultures of human pluripotent stem cells. Biomacromolecules 15, 2067–2078.

Kido, Y., Matsson, Pr, Giacomini, K.M., 2011. Profiling of a prescription drug library for potential renal drug–drug interactions mediated by the organic cation transporter 2. J. Med. Chem. 54, 4548–4558.

Kim, B.S., Putnam, A.J., Kulik, T.J., Mooney, D.J., 1998. Optimizing seeding and culture methods to engineer smooth muscle tissue on biodegradable polymer matrices. Biotechnol. Bioeng. 57, 46–54.

Kirk, A., Campbell, S., Bass, P., Mason, J., Collins, J., 2010. Differential expression of claudin tight junction proteins in the human cortical nephron. Nephrol., Dial., Transplant.: Off. Publ. Eur. Dial. Transpl. Assoc. – Eur. Ren. Assoc. 25, 2107–2119.

Krieter, D.H., Hackl, A., Rodriguez, A., Chenine, L., Moragues, H.L., Lemke, H.D., Wanner, C., Canaud, B., 2009. Protein-bound uraemic toxin removal in haemodialysis and post-dilution haemodiafiltration. Nephrol. Dial. Transplant. 25, 212–218.

Lee, H., Dellatore, S.M., Miller, W.M., Messersmith, P.B., 2007. Mussel-inspired surface chemistry for multifunctional coatings. Science 318, 426–430.

Li, Z., Cui, Z., 2014. Three-dimensional perfused cell culture. Biotechnol. Adv. 32, 243–254.

Meyer, T.W., Walther, J., Pagtalunan, M.E., Martinez, A., Torkamani, A.L.I., Fong, P., Recht, N., Robertson, C., Hostetter, T., 2005. The clearance of protein-bound solutes by hemofiltration and hemodiafiltration. Kidney Int. 68, 867–877.

Ni, M., Teo, J.C., Ibrahim, M.S., Zhang, K., Tasnim, F., Chow, P.Y., Zink, D., Ying, J.Y., 2011. Characterization of membrane materials and membrane coatings for bioreactor units of bioartificial kidneys. Biomaterials 32, 1465–1476.

Oo, Z.Y., Kandasamy, K., Tasnim, F., Zink, D., 2013. A novel design of bioartificial kidneys with improved cell performance and haemocompatibility. J. Cell. Mol. Med. 17, 497–507.

Oo, Z.Y., Deng, R., Hu, M., Ni, M., Kandasamy, K., bin Ibrahim, M.S., Ying, J.Y., Zink, D., 2011. The performance of primary human renal cells in hollow fiber bioreactors for bioartificial kidneys. Biomaterials 32, 8806–8815.

Saito, A., Sawada, K., Fujimura, S., 2011. Present status and future perspectives on the development of bioartificial kidneys for the treatment of acute and chronic renal failure patients. Hemodial. Int. Int. Symp. Home Hemodial. 15, 183–192.
Saito, A., Sawada, K., Fujimura, S., Suzuki, H., Hirukawa, T., Tatsumi, R., Kanai, G., Takahashi, H., Miyakogawa, T., Sanechika, N., Fukagawa, M., Kakuta, T., 2012. Evaluation of bioartificial renal tubule device prepared with lifespan-extended human renal proximal tubular epithelial cells. Nephrol., Dial., Transplant.: Off. Publ. Eur. Dial. Transpl. Assoc. – Eur. Ren. Assoc. 27, 3091–3099.
Sánchez-Romero, N., Meade, P., Giménez, I., 2016. Chapter 22 – Microfluidic-Based 3D Models of Renal Function for Clinically Oriented Research A2 – Laurence, Jeffrey, Translating Regenerative Medicine to the Clinic. Academic Press, Boston, pp. 315–334.
Sanechika, N., Sawada, K., Usui, Y., Hanai, K., Kakuta, T., Suzuki, H., Kanai, G., Fujimura, S., Yokoyama, T.A., Fukagawa, M., Terachi, T., Saito, A., 2011. Development of bioartificial renal tubule devices with lifespan-extended human renal proximal tubular epithelial cells. Nephrol., Dial., Transplant.: Off. Publ. Eur. Dial. Transpl. Assoc. – Eur. Ren. Assoc. 26, 2761–2769.
Schophuizen, C.M., Wilmer, M.J., Jansen, J., Gustavsson, L., Hilgendorf, C., Hoenderop, J.G., van den Heuvel, L.P., Masereeuw, R., 2013. Cationic uremic toxins affect human renal proximal tubule cell functioning through interaction with the organic cation transporter. Pflug. Arch.: Eur. J. Physiol. 465, 1701–1714.
Schophuizen, C.M., De Napoli, I.E., Jansen, J., Teixeira, S., Wilmer, M.J., Hoenderop, J. G., Van den Heuvel, L.P., Masereeuw, R., Stamatialis, D., 2015. Development of a living membrane comprising a functional human renal proximal tubule cell monolayer on polyethersulfone polymeric membrane. Acta Biomater. 14, 22–32.
Shitara, Y., Horie, T., Sugiyama, Y., 2006. Transporters as a determinant of drug clearance and tissue distribution. Eur. J. Pharm. Sci. 27, 425–446.
Tahara, H., Kusuhara, H., Endou, H., Koepsell, H., Imaoka, T., Fuse, E., Sugiyama, Y., 2005. A species difference in the transport activities of H2 receptor antagonists by rat and human renal organic anion and cation transporters. J. Pharmacol. Exp. Ther. 315, 337–345.
Tasnim, F., Deng, R., Hu, M., Liour, S., Li, Y., Ni, M., Ying, J.Y., Zink, D., 2010. Achievements and challenges in bioartificial kidney development. Fibrogenesis Tissue Repair 3, 3–14.
Urakami, Y., 2002. cDNA cloning, functional characterization, and tissue distribution of an alternatively spliced variant of organic cation transporter hOCT2 predominantly expressed in the human kidney. J. Am. Soc. Nephrol. 13, 1703–1710.
Vanholder, R., De Smet, R., Glorieux, G., Dhondt, A., 2003b. Survival of hemodialysis patients and uremic toxin removal. Artif. Organs 27, 218–223.
Vanholder, R., Schepers, E., Pletinck, A., Nagler, E.V., Glorieux, G., 2014. The uremic toxicity of indoxyl sulfate and p-Cresyl sulfate: a systematic review. J. Am. Soc. Nephrol. 25, 1–11.
Vanholder, R., De Smet, R., Glorieux, G., Argiles, A., Baurmeister, U., Brunet, P., Clark, W., Cohen, G., De Deyn, P.P., Deppisch, R., Descamps-Latscha, B., Henle, T., Jorres, A., Lemke, H.D., Massy, Z.A., Passlick-Deetjen, J., Rodriguez, M., Stegmayr, B., Stenvinkel, P., Tetta, C., Wanner, C., Zidek, W., European Uremic Toxin Work, G, 2003a. Review on uremic toxins: classification, concentration, and interindividual variability. Kidney Int. 63, 1934–1943.
Weinbaum, S., Duan, Y., Satlin, L.M., Wang, T., Weinstein, A.M., 2010. Mechanotransduction in the renal tubule. Am. J. Physiol. Ren. Physiol. 299, F1220–F1236.
Wilmer, M.J., Saleem, M.A., Masereeuw, R., Ni, L., van der Velden, T.J., Russel, F.G., Mathieson, P.W., Monnens, L.A., van den Heuvel, L.P., Levtchenko, E.N., 2010. Novel conditionally immortalized human proximal tubule cell line expressing functional influx and efflux transporters. Cell Tissue Res. 339, 449–457.
Zhang, H., Tasnim, F., Ying, J.Y., Zink, D., 2009. The impact of extracellular matrix coatings on the performance of human renal cells applied in bioartificial kidneys. Biomaterials 30, 2899–2911.
Zolk, O., Solbach, T.F., Konig, J., Fromm, M.F., 2009. Functional characterization of the human organic cation transporter 2 variant p.270Ala > Ser. Drug Metab. Dispos. 37, 1312–1318.